

## Software tools for robust extraction, analysis and visualization of porosities in XCT scans of fiber-reinforced polymers

Christoph HEINZL<sup>1</sup>, Johannes WEISSENBÖCK<sup>1</sup>, Andreas REH<sup>1</sup>, Johann KASTNER<sup>1</sup>,  
Tobias DIERIG<sup>2</sup>, Thomas GÜNTHER<sup>2</sup>,  
Denis KIEFEL<sup>3</sup>, Rainer STÖSSEL<sup>3</sup>,

<sup>1</sup> University of Applied Sciences Upper Austria, Wels, Austria; e-mail:  
{c.heinzl|j.weissenboeck|a.reh|j.kastner}@fh-wels.at

<sup>2</sup> Volumegraphics GmbH, Heidelberg, Germany; e-mail: {guenther|dierig}@volumegraphics.com

<sup>3</sup> Airbus Group Innovations, Munich, Germany; e-mail: {rainer.stoessel|denis.kiefel}@airbus.com

### Abstract

Advanced composite materials such as carbon fiber reinforced polymers (CFRPs) play an increasingly important role in aeronautics with regard to efficiency and economy but also with regard to function integration and flexibility. In order to non-destructively characterize CFRP materials and components, 3D X-ray computed tomography (XCT) is increasingly used as a reference and escalation method.

In this work we are targeting XCT data evaluation for one of the main challenges regarding quality control of CRFPs, which is robust extraction and analysis of pores in 3D as well as the specimen's volume porosity. Pores of CFRPs largely influence the mechanical properties of a specimen such as shear strength. Furthermore, their individual characteristics such as shape, position, volume or size, largely determine whether a component meets the required specifications and is therefore able to fly or whether it needs to be rejected or reworked. For this purpose we apply and demonstrate a part of the technology platform developed within the EU-FP7 QUICOM project ([www.quicom.eu](http://www.quicom.eu)) dedicated to porosity analysis. The presented tools encompass robust pore extraction, characterization of pores, pore classification, and advanced pore and porosity visualization methods.

The presented techniques are demonstrated and applied on CFRP specimens of the QUICOM consortium. The tools and the generated results are tested and verified by an end user. Our findings show that using the QUICOM technology platform for robust porosity analysis facilitates an in-depth-view into the material system which may be integrated into a feedback cycle, in order to control and fine tune the development of novel, tailored CFRP components.

**Keywords:** QUICOM, Aeronautics, industrial 3D X-ray computed tomography, fiber reinforced polymers, CFRP, robust pore extraction, visual analysis

### 1) Introduction and Motivation

The most recent and next generation of aircrafts such as the Airbus A350 XWB, the Boeing 787 Dreamliner or the Bombardier C Series, aim to be made of 50 % or more advanced composite materials [Comp14]. To arrive at these high shares, complex primary structures as well as highly loaded propulsion parts are increasingly manufactured using carbon fiber reinforced polymers (CFRPs). Currently, quality control of CFRPs is mainly carried out using ultrasonic inspections or micro cuts [DM06], both of which are increasingly facing their limits, e.g., regarding shape or size of the components, time consumption, or precision. An advanced non-destructive testing (NDT) method for detailed characterization of CFRPs was found in 3D X-ray computed tomography (XCT), which is to date the most promising technique for non-destructive and fully three-dimensional characterization of composite aeronautic components [iCT2014]. XCT allows to generate a volumetric representation of the complete interior and exterior structure of the specimen as well as of the integrated features in the specimen. Structures such as fibers, pores, inclusions or voids, may be segmented and extracted for further analysis. XCT data analysis provides detailed information on each segmented object such as pore size, surface, volume, shape, and further geometrical information which are of interest for material science and development of new composite structures. Pores can have different shapes and sizes and general distinctions in micro-, spherical-, needle-like-, and tubular pores are very useful. Different laminate structures can have different type

and size of pores. A needle shape of pores can often be found in unidirectional (UD-) laminates and along fibers in bi-diagonal laminate structures too, whereas mainly tubular and spherical pores occur in bi-diagonal (bi-) laminates. These kind of material characteristics are analyzed at several different material datasets.

## 2) Description of Data

*Bi-diagonal laminate samples:* The samples AGI-1 to AGI-7 with a cross section of 4 mm x 4 mm were made from 16 plies of bi-diagonal prepreg (0° / 90° layers) and measured with a voxel size of 20 μm.

*Unidirectional laminate samples:* In addition to the bi-diagonal samples, two unidirectional specimens AGI-IX0 and AGI-IX45 were measured with 10 μm and 20 μm voxel size. These samples with a cross section of 2.9 mm x 5.6 mm were manufactured from 15 plies of UD prepreg.

The measurements were performed on a CT-system with Viscom 160TXD X-ray source with diamond target and 1024<sup>2</sup> pixel PerkinElmer flat panel detector. It is an open system which allows different kinds of acquisition, reconstruction, and data evaluation.

## 3) Methods

### 3.1) Robust Extraction of Pores

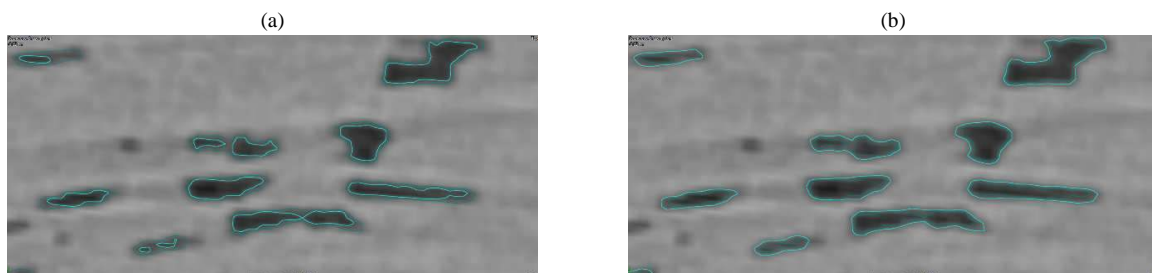
In the following section a new method to calculate absolute porosity of CFRP without the need of using reference samples is described. At the moment, a common and established method in calculating porosity of CFRP is to scan a reference sample with known porosity together with the sample of interest. Based on the reference sample a global threshold to differentiate between pores and fiber/matrix is determined. This global threshold is then used on the sample to get the ratio between pore volume and rest volume, i.e., the porosity. [QNDE10].

However, this method has several disadvantages:

- The need of a scanning a reference sample means extra work, might result in additional artifacts and limits the resolution of the scan.
- Using a global threshold is often not appropriate for real world samples with e.g., varying thickness. Often the same materials may show completely different gray values in a single dataset.
- The results are very sensitive on the threshold chosen.

For many years, Volume Graphics has developed methods to detect and characterize pores and inclusions in XCT data. These algorithms are dealing with common artifacts like beam hardening and scattered radiation, e.g., by using local adaptive thresholds. Therefore there is no need for using a reference sample to determine a global threshold. The relevant information to distinguish between pores and fiber/matrix is extracted from the data itself. Unfortunately these highly advanced algorithms were originally developed for aluminum and plastic castings and do not work out of the box with CFRP data.

So, first of all, in this work we focused on adding a local adaptive correction to the established global threshold based approach. The aim was to get on the one hand rid of using a reference sample for the determination of the global threshold value and, on the other hand, to deal with local grey value variations due to artifacts. The basic idea is to start from the global threshold given pore surface and to detect the real local surface described by maximum gradient. In Figure 1) you can see the effect of the local adaptive correction: Figure 1a) shows the case of a threshold which has been chosen 30% to low, Figure 1c) shows the case of a threshold which is 10% to high. In both cases of wrong threshold values, the pore definition gets corrected in Figure 1b) and Figure 1d).



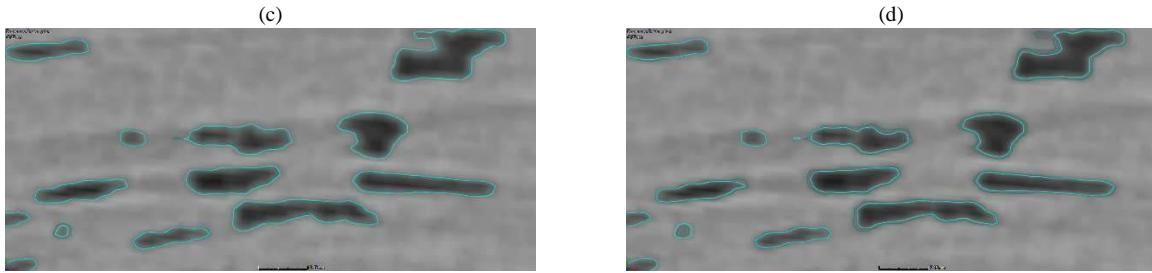


Figure 1) (a) Low Threshold -30% (b) Low Threshold -30% after correction  
(c) High Threshold +10% (d) High Threshold +10% after correction

In Figure 2) we show the effect of reducing the error in global porosity by using the local adaptive correction. For a list of given thresholds we have calculated the relative error in porosity for both with and without local adaptive correction.

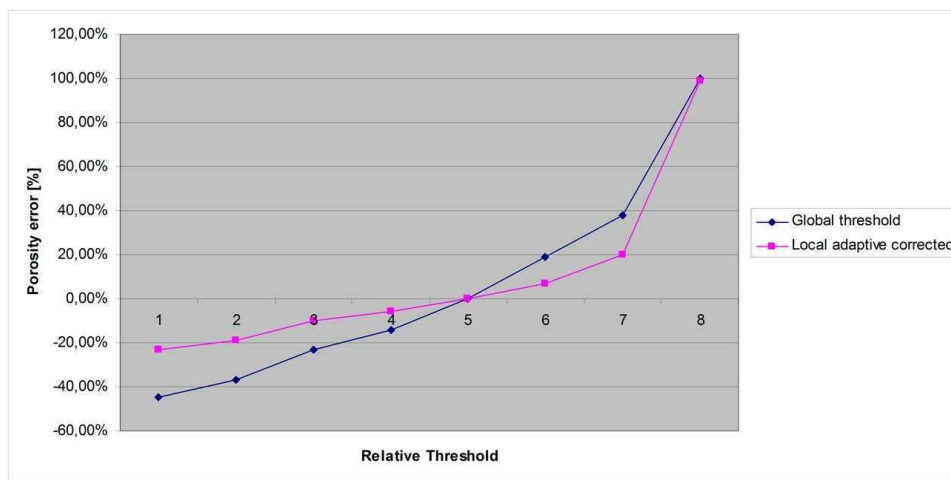


Figure 2) Relative error in porosity with and without local adaptive correction

As a result, we can state that local adaptive correction has a stabilizing effect on the global threshold method and renders it less vulnerable against global or local grey value modifications.

Second, we added methods to define a starting threshold not by scanning a reference sample but by analyzing the grey value data of the scanned part itself. Typically, the threshold can be defined either in relation to the (automatically detected) material and background peaks of the grey value histogram or in relation the material peak and its grey value deviation. Two different modes may be used to determine the starting global threshold:

- Interpolation allows to define the threshold in percent between background peak and material peak.
- Deviation allows to define the threshold as a value relative to the material peak in the unit of a standard deviation of the material grey values.

So, they finally allow to define and calibrate an analysis template independent of the actual grey value range. For similar materials, the user is able to calibrate it once with precise measured reference samples and then use it in a wide range independent of the actual scan parameters. The methods has been tested with several CFK scans from Airbus Group Innovations, showing stable results over a wide range. In the following, results for a high-level porosity probe scanned together with a reference sample is shown:

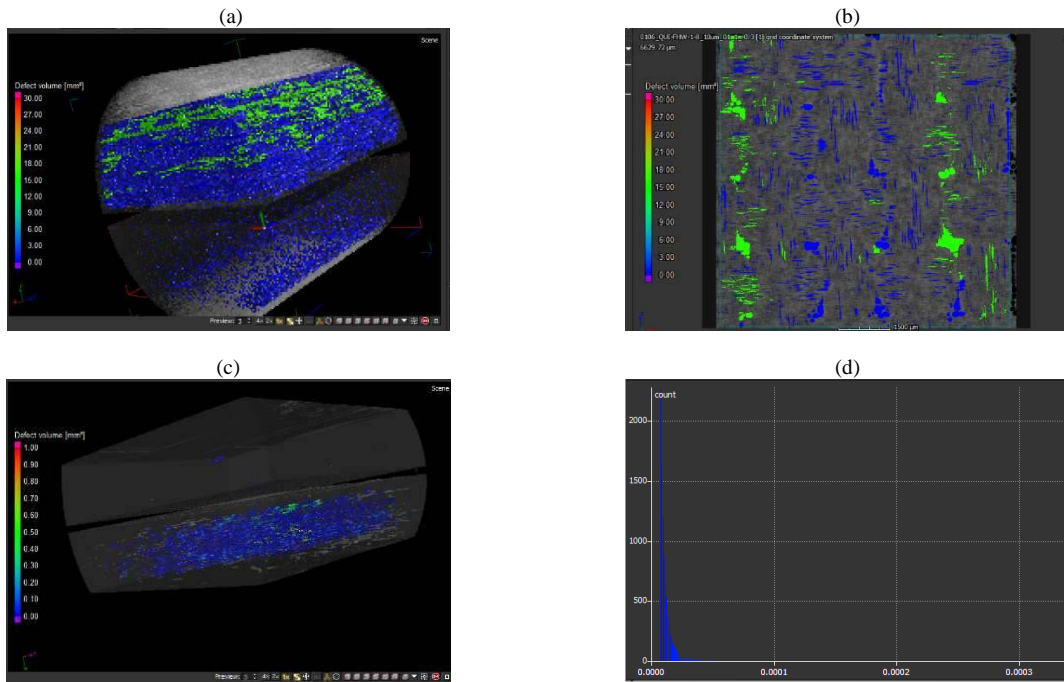


Figure 3) (a) 3d and (b) 2d visualization of high level porosity with color coding of pore volume (c) 3d visualization of medium porosity with color coding of pore volume (d) pore size distribution

Third we focused on the improvement of an advanced algorithm, developed for and established in the field of aluminum and plastic castings. New criteria for both the segmentation and classification steps has been developed to improve the detection of porosity significantly. In Table 1, a comparison of the new VGDefX CFRP method to the reference method is presented on 5 datasets as described in section 2, using the same parameter settings for all datasets. In this table results are also shown combing the new VGDefX CFRP algorithm with local adaptive refinement as described before.

Name	Reference	VG DefX CFRP	VG DefX CFRP + Local Refinement	abs. Difference	rel. Difference
QUI-AGI 3	0,82%	0,82%	0,74%	0,08%	10,00%
QUI-AGI 4	0,70%	0,70%	0,63%	0,07%	10,00%
QUI-AGI 5	6,55%	7,51%	6,49%	-0,06%	-0,01%
QUI-AGI 6	7,04%	7,90%	7,48%	0,44%	6.20%
QUI-AGI 7	7,92%	6,55%	7,66%	-0,26%	-3.20%

Table 1) Comparison of porosity detection methods on 5 QUI-AGI datasets

Finally we focused on the separation of pore clusters to perform on this components an extraction of pore measures like volume, surface, main orientation and form factors. In Figure 4) the result of this fully automated pore cluster separation is depicted.

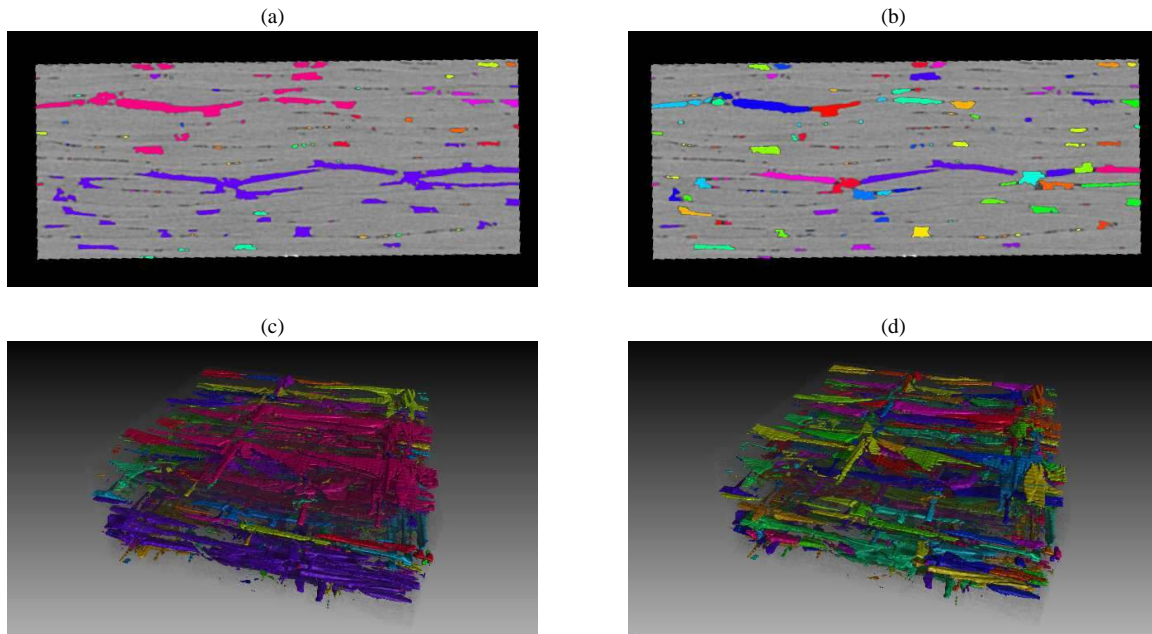


Figure 4) Visualization of pore cluster without (a) + (c) and with (b) + (d) separation. Different colors represent different pores.

### 3.2) Visual Analysis

When evaluating datasets of porous structures the main requirement of the end users besides getting reliable quantitative porosity values is to get insight into the characteristics of the individual pores. Therefore advanced analysis, visualization and exploration methods are essential for an in-depth analysis of the underlying data. In this work we employ three different methods of our previous work [RPK12], [RGK13], [WAL14] incorporated in the iAnalyse tool [iAn14] to address this task: For a general overview of the porosity within the component we calculate maps of the extracted pores on the complete XCT dataset of the specimen. Furthermore, we employ a drill down approach to explore and focus on pores of interest. We finally calculate mean pores of the defined pore classes for further analysis, modelling or simulation.

The first analysis and visualization technique follows the goal to provide the end users with a global overview of the analyzed component regarding the regional distribution of the individual pores within the specimen. Using porosity maps [RPK12], areas of the specimen of high and low porosity are intuitively displayed. Typically, porosity maps are calculated for x, y and z directions by adding all voxels of the segmented pore in the corresponding direction: For each pixel in the porosity map all contributing voxels along the viewing ray are added and stored. The generated porosity map is then colored according to the calculated frequency values of segmented voxels.

To explore the dataset in more detail, we are using the FiberScout tool [WAL14]. FiberScout was designed as an interactive visual analysis tool for the exploration of segmented or labelled structures, extracted from XCT data. The tool first calculates properties of interest for each individual segmented object (e.g., volume, shape factor, position, extents, etc.). The extracted properties are in the second step visualized in parallel coordinates as well as a scatter plot matrix. Using parallel coordinates, those properties of interest are depicted in parallel and equidistant axes. For each segmented object the calculated property values are integrated in the plot and connected using a polyline per object. Parallel coordinates thus allow to show correlations between adjacent properties. Selecting ranges in the parallel coordinates allows for clustering of the segmented objects, marking the selected polylines in red. In order to refine the data exploration a scatter plot matrix is used. The scatter plot matrix is an arrangement of individual scatter plots, each of those plotting a property of interest over another. The segmented objects are represented in the scatter plots as single dot. Selected objects are again marked as red dot. Using brushing the user may refine the initial classification using each scatter plot. Both parallel coordinates as well as a scatter plot matrix are linked to 2D slicers as well as the 3D view, indicating the selected objects in red color. As soon as the user has finished his refinement, a new class of segmented objects may be created and stored in the class explorer view.

As it is desired by the end users to investigate the mean representation of objects, the datasets are analyzed by a second technique using a method to calculate mean objects for a class of interest [RGK13]. The calculation of the mean representation was coupled to the FiberScout tool allowing to calculate individual mean representations for each of the defined classes of segmented objects. The used mean objects approach first aligns the individual

objects. Then the individual segmented objects are added on voxel basis. In this step each occurrence (i.e. each voxel) of a segmented object contributes to the resulting mean representation. Considering the total number of individual segmented objects a statistical representation of the mean object may be computed. A 3D view allows for visualizing the mean representation using transfer functions. For further analysis as well as for detailed component simulation, iso-probability surfaces of the mean representation may be extracted.

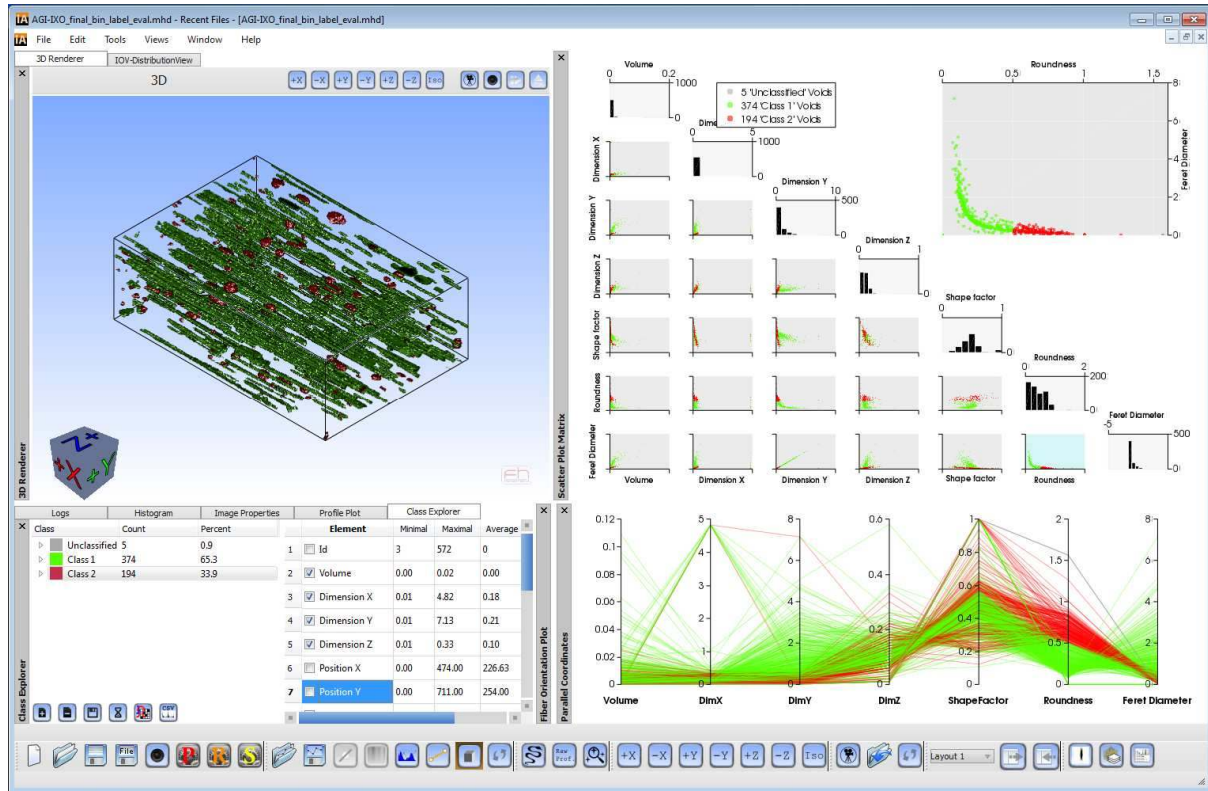


Figure 5) iAnalyze data analysis and visualization framework. 3D view renderer (top left), Class explorer (bottom left), Scatterplot matrix (top right) and Parallel coordinates (bottom right). The selected individual objects are rendered in red and linked between all views for interactive data exploration (FHW replace, QUICOM dataset).

#### 4) Results and Evaluation

For the analysis of pore shape and geometry with iAnalyze, three different CFRP samples were chosen: Two unidirectional prepreg samples in which often needle-like pores occur and bi-diagonal prepreg samples in which tubular and spherical pores mainly appear. Those different pore shapes can be evaluated and separated from each other to obtain information which is useful in material research and mechanical stress analysis. Therefore, the pores were extracted by using the robust extraction method of VGStudioMax and afterwards evaluated by using iAnalyze.

There are many options available to separate pores for generating pore-classes. The most significant difference between needle-like and spherical pores is their general roundness. Figure 6a) shows a dataset of sample AGI-IX0 with a voxel size of 10  $\mu\text{m}$ . The roundness of its needle-like pores was defined to be between 0.0 and 0.5, as depicted in Figure 6b). The spherical pores were defined to have a roundness  $> 0.5$  (Figure 6c)). Furthermore, for these two classes, mean objects [RGK13] were calculated. Figure 6d) visualizes on the left side in blue the average pore shape for needle-like pores, and in yellow their deviation. Same visualization for spherical pores is shown on the right.

The bi-diagonal CFRP samples with mainly tubular and spherical pores were separated in two classes by using the roundness characteristic too, however, with a threshold of 0.6. Figure 6e) depicts the analyzed dataset with a voxel size of 21  $\mu\text{m}$  and in Figure 6f) and 6g) their separated classes. There is a significant difference recognizable in the MObject visualization, even though the pore shapes itself do not differ significantly as e. g. in UD-laminates.

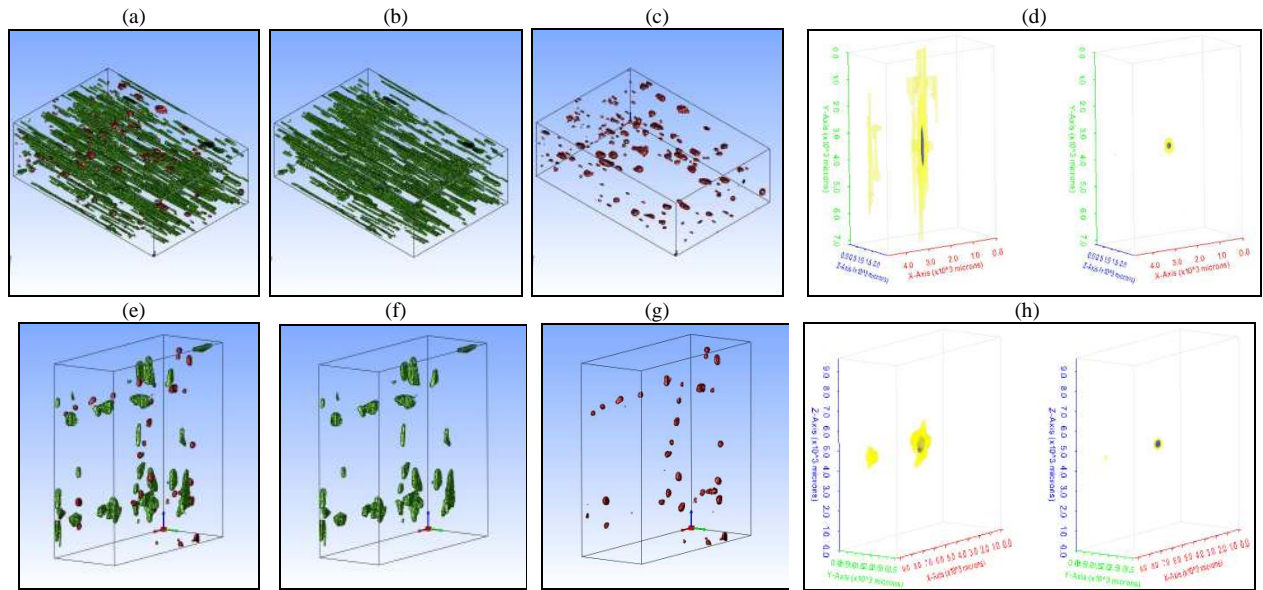


Figure 6 (a) UD-laminate sample AGI-IX0 which was separated in (b) needle-like and (c) spherical pores and their (d) Mean object visualization. (e) bi-diagonal sample AGI-3 with (f) tubular pore, (g) spherical pore separation and (h) Mean object visualization.

Furthermore, it is possible to evaluate the orientation of pores. Therefore, the sample AGI-IX45, which is made of the same laminate as AGI-IX0, was cut-out with  $45^\circ$  related to the fiber orientation in order to evaluate the pore orientation by using the advantage of needle-like pores shape (Figure 7a) and 7b)). The evaluated orientation is shown in Figure 7c), where normalized frequency distributions of analyzed orientations are plotted against the angle.

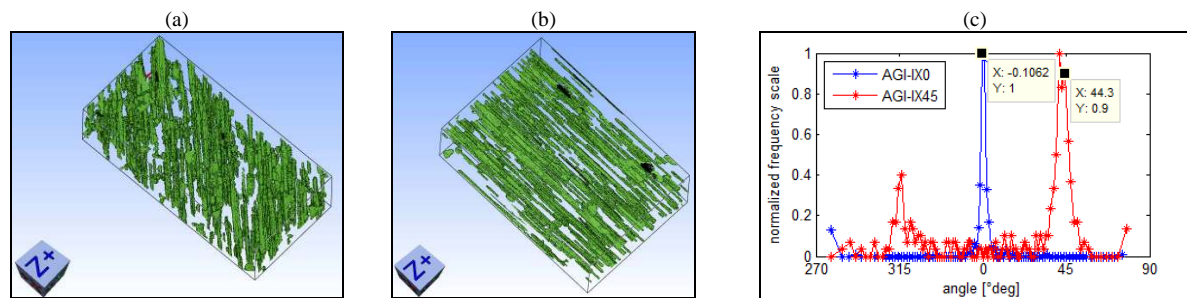


Figure 7 (a) Dataset AGI-IX45 with  $45^\circ$  cut orientation related to fiber orientation and (b) AGI-IX0 with  $0^\circ$  cut direction. (c) Normalized frequency distributions of evaluated pore orientations.

## 5) Conclusions and future work

For the robust extraction of pores we could show that it is possible to become widely independent from scanning reference samples. The generated results are comparable to the reference method. Just by using information from the scan itself, it has been possible to reproduce at a great extend the results from the reference method. Using the proposed analysis tool the evaluation of pore shape and separation of pores by using specific pore characteristics like the roundness worked out very well. It is possible to get detailed information about pore geometry and to compare characteristics with each other. Furthermore, mean representations can be calculated which visualizes average pore shapes and deviations to it. Additionally, it is possible to evaluate the orientation of pores, which can be interesting for fiber orientation analysis in CFRP materials where fiber/resin contrast is too low for standard evaluation. For future work we are planning to test the tool on further samples. It is planned to further improve the precision of the robust pore extraction as well as to extend the functionality of the analysis tools.

## Acknowledgements

This project was supported by the QUICOM project, which is financed by the European Union Seventh Framework Programme (FP7/2007- 2013) under Grant Agreement no 314562.

## References

- [QNDE10] R.Stoessel, T.Guenther,T.Dierig,  $\mu$ -Computed Tomography for micro-structure characterization of CFRP, QNDE 2010, San Diego, California
- [Comp14] Compositesworld: Aviation outlook. <http://www.compositesworld.com/articles/aviation-outlook-fuel-pricing-ignites-demand-for-composites-in-commercial-transports> last visited May 25<sup>th</sup>, 2014
- [ICT14] J. Kastner (Editor) Proceedings of Conference on Industrial Computed Tomography 2014, Wels, Austria, 2014
- [WAW14] Weissenböck J., Amirkhanov A., Weimin Li, Reh A., Amirkhanov A., Gröller E, Kastner J., Heinzl C.; FiberScout: An Interactive Tool for Exploring and Analyzing Fiber Reinforced Polymers; Pacific Visualization Symposium (PacificVis); 2014 IEEE; pp.153-160; 4-7 March 2014; doi: 10.1109/PacificVis.2014.52
- [RGK13] A. Reh, C. Gusenbauer, J. Kastner, E. Gröller, C. Heinzl, MObjects - A Novel Method for the Visualization and Interactive Exploration of Defects in Industrial XCT Data, In IEEE Transactions on Visualization and Computer Graphics (TVCG), Vol. 19, No. 12, 2013, pp. 2906-2915
- [RPK12] A. Reh, B. Plank, J. Kastner, E. Gröller, C. Heinzl, Porosity Maps: Interactive Exploration and Visual Analysis of Porosity in Carbon Fiber Reinforced Polymers using X-Ray Computed Tomography, In COMPUTER GRAPHICS FORUM, Vol. 31, No., 3, 2012, pp. 1185-1194
- [DM06] N. Dominguez, B. Mascaro, Ultrasonic Non-Destructive Inspection of Localised Porosity in Composite Materials, European Conference on Non-Destructive Testing, Berlin, Germany, 2006